• Basic Research •

Effects of *Lycium barbarum polysaccharide* on the photoinduced autophagy of retinal pigment epithelium cells

Yuan-Yuan Gao[1,2], Juan Li[1], Jie Huang[1], Wu-Jun Li[2], Yang Yu[1]

[1]Ningxia Medical University, Yinchuan 750004, Ningxia Hui Autonomous Region, China
[2]Yulin Hospital of Traditional Chinese Medicine, Yulin 719000, Shaanxi Province, China
Correspondence to: Yang Yu. Ningxia Medical University, Yinchuan 750004, Ningxia Hui Autonomous Region, China. 20070030@nxmu.edu.cn
Received: 2021-07-01 Accepted: 2021-09-09

Abstract

● **AIM:** To investigate the relationship between autophagy and apoptosis in photoinduced injuries in retinal pigment epithelium (RPE) cells and how *Lycium barbarum polysaccharide* (LBP) contributes to the increased of RPE cells to photoinduced autophagy.

● **METHODS:** *In vitro* cultures of human RPE strains (ARPE-19) were prepared and randomly divided into the blank control, model, low-dose LBP, middle-dose LBP, high-dose LBP, and 3-methyladenine (3MA) groups. The viability of the RPE cells and apoptosis levels in each group were tested through cell counting kit-8 (CCK8) method with a flow cytometer (Annexin V/PI double staining technique). The expression levels of LC3II, LC3I, and P62 proteins were detected with the immunofluorescence method. The expression levels of beclin1, LC3, P62, PI3K, P-mTOR, mTOR, P-Akt, and Akt proteins were tested through Western blot.

● **RESULTS:** LBP considerably strengthens cell viability and inhibits the apoptosis of RPE cells after photoinduction. The PI3K/Akt/mTOR signal pathway is activated because of the upregulation of the phosphorylation levels of Akt and mTOR proteins, and thus autophagy is inhibited.

● **CONCLUSION:** LBP can inhibit the excessive autophagy in RPE cells by activating the PI3K/Akt/mTOR signaling pathways and thereby protect RPE cells from photoinduced injuries.

● **KEYWORDS:** autophagy; *Lycium barbarum polysaccharide*; retinal pigment epithelial cell; photoinduced apoptosis
DOI:10.18240/ijo.2022.01.04

Citation: Gao YY, Li J, Huang J, Li WJ, Yu Y. Effects of *Lycium barbarum polysaccharide* on the photoinduced autophagy of retinal pigment epithelium cells. *Int J Ophthalmol* 2022;15(1):23-30

INTRODUCTION

Age-related macular degeneration (AMD) is a disease characterized by degenerative changes and angiogenesis in photoreceptors in the retinal macular zone and retinal pigment epithelium (RPE). It is a major chronic disease that causes blindness in aged people and greatly reduces not only their quality of life but also that of their families. Stimulated under certain conditions and influenced by autolysosomes or autophagy vesica, autophagy provides substances essential to basic cell survival by degrading and eliminating subcellular fragments[1-2]. The role of autophagy in the optical injuries of the retina is controversial. Autophagy disorder can induce the apoptosis of RPE cells[3], and inhibiting autophagy can prevent light-induced damage to photoreceptors[4]. Therefore, elaborating the role and action mechanism of autophagy in photoinduced retinal injuries and searching an effective therapeutic strategy for AMD are necessary.

Lycium barbarum polysaccharide (LBP) is a major bioactive component of Chinese wolfberry fruit and is a protein polysaccharide composed of monosaccharides, such as arabinose, rhamnose, xylose, mannose, galactose, and glucose[5]. Modern pharmacological studies have demonstrated that LBP has antioxidative, anti-aging, immunoregulatory, and antifatigue functions, provides protection against radiation, and protects the reproductive system[6]. In ocular regions, LBP can protect ganglion cells from retinal ischemic and reperfusion injuries[7], exerts neuroprotective effects in acute and chronic intraocular hypertension rat models[8], plays an important role in the antioxidative stress pathway[9-10], and protects photoinduced retina models[11-12].

In previous studies, we have found that the fruit of Chinese wolfberry can protect RPE cells to some extent possibly through antioxidative stress and by regulating Bcl2/Bax protein expression ratio and inhibiting mitochondrial and endoplasmic reticulum apoptosis signal transduction pathway.

The principles underlying the roles of Chinese wolfberry fruit in "tonifying kidney and improving eyesight" have been elaborated[10-16]. To elucidate how LBP protects human RPE cells from photoinduced injuries during the photoinduced autophagy of RPE cells, we discuss the relationship between autophagy and apoptosis on the basis of cellular morphology and proteomics. This study is expected to provide new insights into AMD prevention and methods decreasing the risk of AMD and facilitate the development of natural drugs for AMD.

MATERIALS AND METHODS

Experimental Materials ARPE-19 was bought from China Beena Biological Company.

Main Reagents and Instruments The main reagents included fetal calf serum (Bioind Company, Israel), Dulbecco's modified Eagle medium (DMEM)/F12 (Bioind Company, Israel), cell counting kit-8 (CCK8) detection kit (Shanghai Beibo Biotechnology Co., Ltd., China), annexinV-FITC apoptosis detection kit (Shanghai Bebo Biotechnology Co., Ltd., China), BC protein quantification kit, whole protein extraction kit (Jiangsu Kaiji Biotech Co., Ltd., China), LC3I-specific antibody, LC3II-specific antibody, and P62/SQSTM1 antibody (all bought from Wuhan Sanying Biotech Co., Ltd., China); rabbit anti-beclin 1 antibody, rabbit anti-PI3 kinase p110 beta antibody, Akt antibody, Akt-phospho-S473 antibody, rabbit anti-phospho-mTOR antibody (all puchased from Proteintech, China-US joint venture), 3-methyladenine (3MA; Apexbio Technology LLC, USA). The major instruments included Multiskan ELISA (Thermo Company, USA), FACSAriaII flow cytometer (BD Company, USA), and TES-1332A digital illuminometer (TaiBei TASS Electronics Industries, China), transmission electron microscopy (H7800, Hitachi, Japan).

Cell Culture All cells were incubated in a humidified incubator at 37℃ with 5% CO_2. ARPE-19 cells were incubated in a humidified incubator at 37℃ with 5% CO_2, and the liquid was changed every other day. When cell density increased to 80%-90%, the cells were digested and passed on in a ratio of 1:3. The third to sixth generations of the cells in the logarithmic phase were selected. Cell suspension was incubated into a 96-well culture plate at a concentration of 1×10^4 cells/well (100 μL per well). The plate was placed in an incubator at 37℃ and 5% CO_2 for 12h, and the experiment was started after cell adherence. The experimental samples were divided into five groups: ARPE-19 cell group (control group), ARPE-19 cell + illumination group (model group), ARPE-19 cells + illumination for the first 2h + autophagy inhibitor 3MA group (3 mmol/mL), ARPE-19 cells + illumination for the first 2h + LBP low-dose group (10 mg/L), ARPE-19 cells + illumination for the first 2h + LBP middle-dose group (50 mg/L), and ARPE-19 cells + illumination for the first 2h + LBP high-dose group (100 mg/L). Indexes were tested after illumination for 24h.

Establishing a Photoinduced Injury Model of Human RPE Cells The third to sixth generations of ARPE-19 cells in the logarithmic phase were selected and cultured in a 6-well plate in a closed incubator under illumination without natural light interference. A three-primary-color light-emitting diode cold light lamp was used as the light source. It was hung at the top of the incubator for straight illumination. According to previous experimental results[17], the illuminometer was used in monitoring illumination strength. The illumination strength of the cells was controlled at 16500±500 lx, and the illumination time was 24h. During illumination, temperature fluctuations in the cell plane were controlled between 36.5℃ and 37.5℃. This procedure eliminated the possibility of photoinduced injuries at increasing temperature.

Observing Cell Ultrastructural Effects Through Transmission Electron Microscopy ARPE-19 cells with a good growth state were used for experiments. The original culture solution was discarded after illumination, then washed and stored at 4℃ for 20min in a refrigerator. The cells were then transferred to a 15 mL centrifuge tube and centrifuged at 1000 rpm/min in a horizontal rotor centrifuge for 10min. The cells were allowed to settle, mixed with 1 mL of glutaraldehyde, and left to stand at 4℃ for 30min in the refrigerator. The cells were centrifuged again, allowed to settle, mixed with 2 mL of buffer, and left to stand at 4℃ for 30min in the refrigerator (repeated three times). The cells were soaked in 1% sour for 1h, and the the buffer was rinsed twice for 15min each. Ultra-thin slices were prepared by dehydrating the cells with increasing concentrations of alcohol , gradually penetrated with epoxy resin, and fixed with acetate. The sections were stained with citrate, and cell ultrastructure was observed through transmission electron microscopy (TEM).

Cell Survival Rate Detection Based on the CCK8 The second to fourth generations of ARPE-19 cells in the logarithmic phase were inoculated into a 96-well plate after digestion at a density of approximately 5×10^3 cells/well. The cells were starved in media without fetal calf serum overnight in an incubator. All groups were terminated from culture at the end of illumination, and the old media were eliminated through absorption. Then, 100 μL of preheated new media were added to each well (containing 10 μL of CCK8 solution) and incubated under 37℃ for 2.5h. The 96-well plate had three replicates of holes for each group, and a control group was set. The optical density (OD) of each hole at 450 nm was detected through ELISA. The experiment was repeated three times. According to mean±standard deviation, data were calculated, and a cell survival rate diagram was drawn. Cell survival rate was calculated as follows: [(OD of cells with drugs–OD of blank control group)/(OD of control cells–OD of blank cells)] ×100%.

Cell Apoptosis Rate Test Based on Flow Cytometery ARPE-19 cells grew well, and cells in the logarithmic phase were selected as experimental samples. After illumination treatment, all groups were processed, and the old culture solution was collected and then rinsed with warm phosphate buffer saline (PBS) two or three times. The cells were digested with 0.25% pancreatin without ethylene diamine tetraacetic acid (EDTA) and phenol red. The cells were mixed evenly for the preparation of a single-cell suspension. The suspension was transferred to a centrifuge tube, and then centrifuged for 5min at a rotation rate of 1200 rpm/min. The supernate was eliminated, and residues were rinsed with 2 mL of PBS once, mixed evenly, and finally used in preparing a single-cell suspension. The suspension was centrifuged again for 5min at a rotation rate of 1200 rpm/min, and the supernate was eliminated. The process was repeated twice. The cells were suspended in 400 μL of annexin-V binding buffer, and 5 μL of FITC was added under the dark. The mixture was left to stand for 15min under 4℃. Subsequently, 10 μL of proteinase inhibitor was added in the dark for 5min before the loading, and flow cytometry was accomplished in 1h.

LC3II, LC3I, and P62 Protein Expression Level Detection Through Immunofluorescence The solution containing the third to fourth generations of ARPE-19 cells in the logarithmic phase were collected for hepatocytes growing on glass coverslips at a density of 6×10^5 cells/piece. The cells were mixed evenly and cultured for 48h. Drugs were added according to different groups, and 24h of illumination was provided after 2h. Cells were collected and rinsed with PBS three times, fixed with 4% paraformaldehyde for 30min, and stored at 4℃. The samples were then rinsed three times (3min each) and then incubated for 15min in 3% endogenous blocker hydrogen peroxide under 37℃. The samples were subsequently washed with PBS three times for 3min each. A working solution of goat serum was added, and the mixture was incubated for 30min at 37℃. The primary antibody was added, and the solution was left to stand at 4℃ overnight. Subsequently, the cells were warmed for 1h at 37℃ and rinsed with PBS three times for 10min each. The second antibody was added dropwise, and the solution was incubated for 30min at 37℃ before rinsing with PBS three times for 5min each. The samples were treated with DAB for 2-3min, and excessive deep colors were prevented. Then, the samples were re-stained with hematoxylin for 3min. The gradient dehydration of alcohol and dripping of neutral vegetable glue were performed. Finally, glass coverslips were sealed.

Beclin1, LC3, P62, PI3K, P-mTOR, mTOR, P-Akt, and Akt Protein Expression Level Detection Through Western Blot Proteins in the cells of each group were extracted using protein lysates, and protein quantification was performed with a BCA quantitative determination kit. Specifically, 50 μg of each sample was loaded through degeneration after computer adjustment. The samples were transferred to a PVDF transmembrane after SDS-PAGE electrophoresis, and the primary antibody was added. The mixture was mixed with 5% skim milk powder for 2h, sealed overnight at 4℃, rinsed with tris buffered saline tween (TBST) three times (10min), mixed with the second antibody, and incubated in a shaker at 37℃ for 2h. A luminescent solution was added in a dark room for exposure. After X-ray development and photographic fixing, the gray values of the protein stripes were analyzed with Image J. The gray values of different protein stripes were quantitatively analyzed, and β-actin was used as the internal reference. A histogram was drawn, and data were expressed as mean±standard deviation (n=3).

Statistical Analysis SPSS 21.0 or Graphpad Prism 6.0 was used in statistical analysis. Data were expressed as mean±standard deviation(s). The normal distribution of data was tested. One-factor ANOVA was used for data comparison, which conformed to normal distribution and homogeneity of variance. Multiple comparisons of several sample means were tested with the SNK-Q method, and the significance level was determined at 0.05 (α=0.05).

RESULTS

Photoinduced Autophagy of ARPE-19 Cells The morphology of autophagosomes in the ARPE-19 cells was observed through TEM (Figure 1). Typical dual-membraniform autophagosomes and autophagy characteristics were observed. Autophagosomes and autolysosomes were hardly observed in the control group. These results indicated that illumination can induce autophagy in ARPE-19 cells.

LBP Inhibits the Photodamage-mediated Deaths of ARPE-19 Cells Figure 2 shows that the cell survival rates of the model group after 24h of photodamage (16500±500 lx) decreased significantly compared with that of the control group (P<0.01). The cell survival rates of the 3MA groups and the LBP-L, LBP-M, and LBP-H groups with photodamage increased compared with the cell survival rate of the model group (P<0.01). A certain intensity of photodamage can considerably decreased cell survival rate, and modeling was successful. LBP increased the survival rate of RPE cells in a dose-dependent manner and protected RPE cells from photodamage.

LBP Inhibits the Photoinduced Apoptosis of ARPE-19 Cells Figure 3 shows that the apoptosis level of the model group increased dramatically compared with that of the control group (P<0.01) and the apoptosis level of the 3MA group decreased compared with that of the model group (P<0.01). The apoptosis levels of the ARPE-19 cells in the LBP-L, LBP-M, and LBP-H groups were lower than the apoptosis level of the model group (P<0.01). These results indicated that LBP can

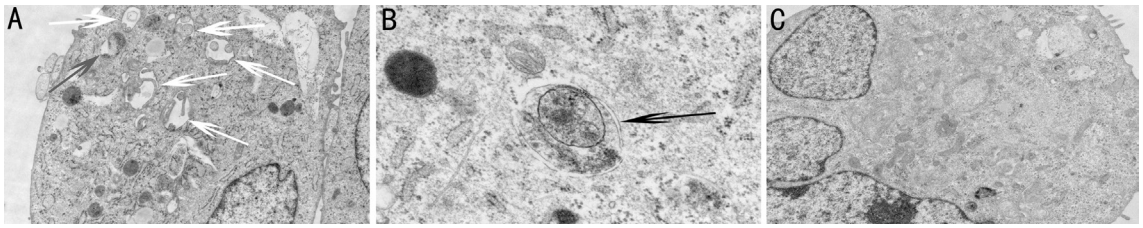

Figure 1 Ultrastructural changes in ARPE-19 cells were observed by TEM A: Model group ×5000; B: Model group ×20 000; C: Control group ×5000. The white arrows point to cytosol substances, including organelles, which were isolated within dual-membrane bonded vesicles. The black arrows are typical of double-membrane autophagosomes.

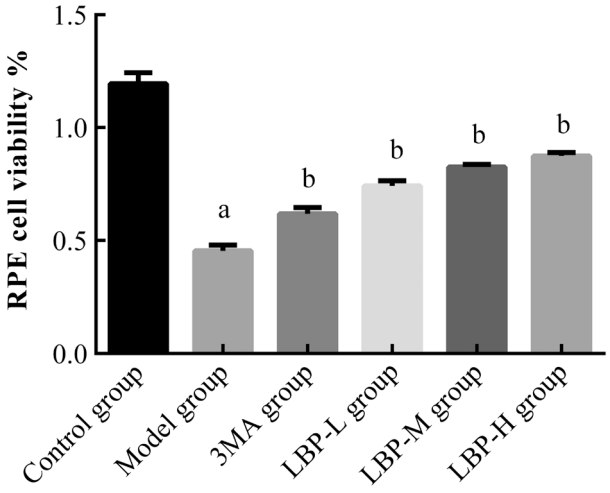

Figure 2 LBP inhibits the photodamage-mediated deaths of ARPE-19 cells [a]Compared with the control group, $P<0.01$; [b]Compared with the model group, $P<0.01$.

inhibit the photoinduced apoptosis of ARPE-19 cells and its ability to inhibit apoptosis is positively related to its concentration.

LBP Inhibits Photoinduced Autophagy in RPE Cells LC3 and P62 proteins were located in the cytoplasm and appear as claybank particles after staining. The immunofluorescence method was used to detect the staining degree of LC3II, LC3I, P62 before and after photoinduced authophagy and after intervention with different concentrations of LBP. These results indicated that LBP inhibits autophagy and increases cell survival rate (Figure 4).

LBP Inhibits Photoinduced Autophagy in ARPE-19 Cells As shown in Figure 5, the expression levels of beclin1 and LC3 in the model group increased compared with those of the control group, LC3II/LC3I level increased and P62 expression level was low. These results indicated that autophagy was activated to a higher degree in the model group than that in the control group. In other words, illumination induced autophagy and increased autophagy flux. After intervention with different concentrations of LBP, the expression levels of beclin1 and LC3II, which were proteins related to photoinduced autophagy, and LC3II/LC3I decrease, whereas the expression level of P62 increased. The expression levels of beclin1, LC3II and LC3II/LC3I were negatively related to LBP concentration, whereas the expression level of P62 was positively related to LBP concentration. These results showed that LBP can inhibit photoinduced autophagy in ARPE-19 cells. The LBP-H group (100 mg/L) shows a higher degree of autophagy inhibition in ARPE-19 cells than the LBP-L group (10 mg/L).

LBP Activates the PI3K/AKt/mTOR Signal Pathway Figure 6 shows that the expression levels of PI3K, P-mTOR, and P-Akt, which were proteins related to the proliferation pathway in the model group, decrease after 24h of illumination compared with those in the control group ($P<0.01$). Similarly, P-mTOR/mTOR and P-Akt/Akt ($P<0.01$) were reduced. The expression levels of PI3K, P-mTOR, and P-Akt in the LBP-L, LBP-M, and LBP-H groups increased compared with those in the model group ($P<0.01$). P-mTOR/mTOR and P-Akt/Akt levels are also increased ($P<0.01$). We concluded that LBP may promotes the phosphorylation of mTOR and Akt, induces the activation of the PI3K/Akt/mTOR signal pathway, and inhibits the expression of beclin1 and LC3II.

3MA Inhibits the Autophagy of RPE Cells According to Figure 7, the 3MA group had a lower expression level of beclin1 in the ARPE-19 cells after 24h of illumination than the model group ($P<0.01$), and the LC3II/LC3I decreases ($P<0.01$), but the expression level of P62 was increased ($P<0.05$). The expression level of beclin1 was higher than that in the control group ($P<0.01$), and LC3II/LC3I level increased slightly ($P<0.05$). The P-mTOR/mTOR level of the 3MA group was higher than that of the model ($P<0.05$) but lower than that of the control group ($P<0.01$). These result indicateed that autophagy activated by illumination in the 3MA group was inhibited after the upregulation of P-mTOR.

DISCUSSION

Autophagy is conducive to the maintenance of steady balance and metabolic adaptation of normal tissues and is an indispensable biological process. However, excessive autophagy has serious consequences[18]. Autophagy eliminates lipid peroxides in RPE cells[19] and is extremely active in RPE and photoreceptor cells. Moreover, impaired autophagy might lead to the early degradation of RPE cells[20]. The physiological functions of RPE can be associated with autophagy in age-related retinal diseases and photoinduced retinal degenerative diseases, such

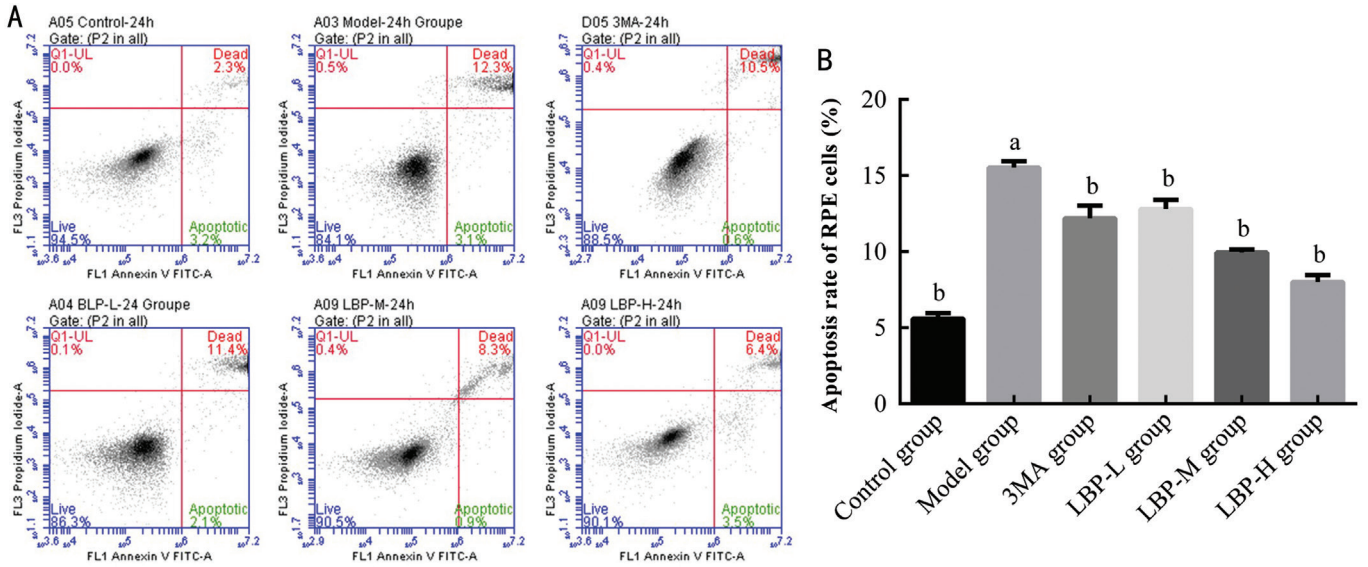

Figure 3 LBP inhibits the photoinduced apoptosis of ARPE-19 cells [a]Compared with the control group, $P<0.01$; [b]Compared with the model group, $P<0.01$.

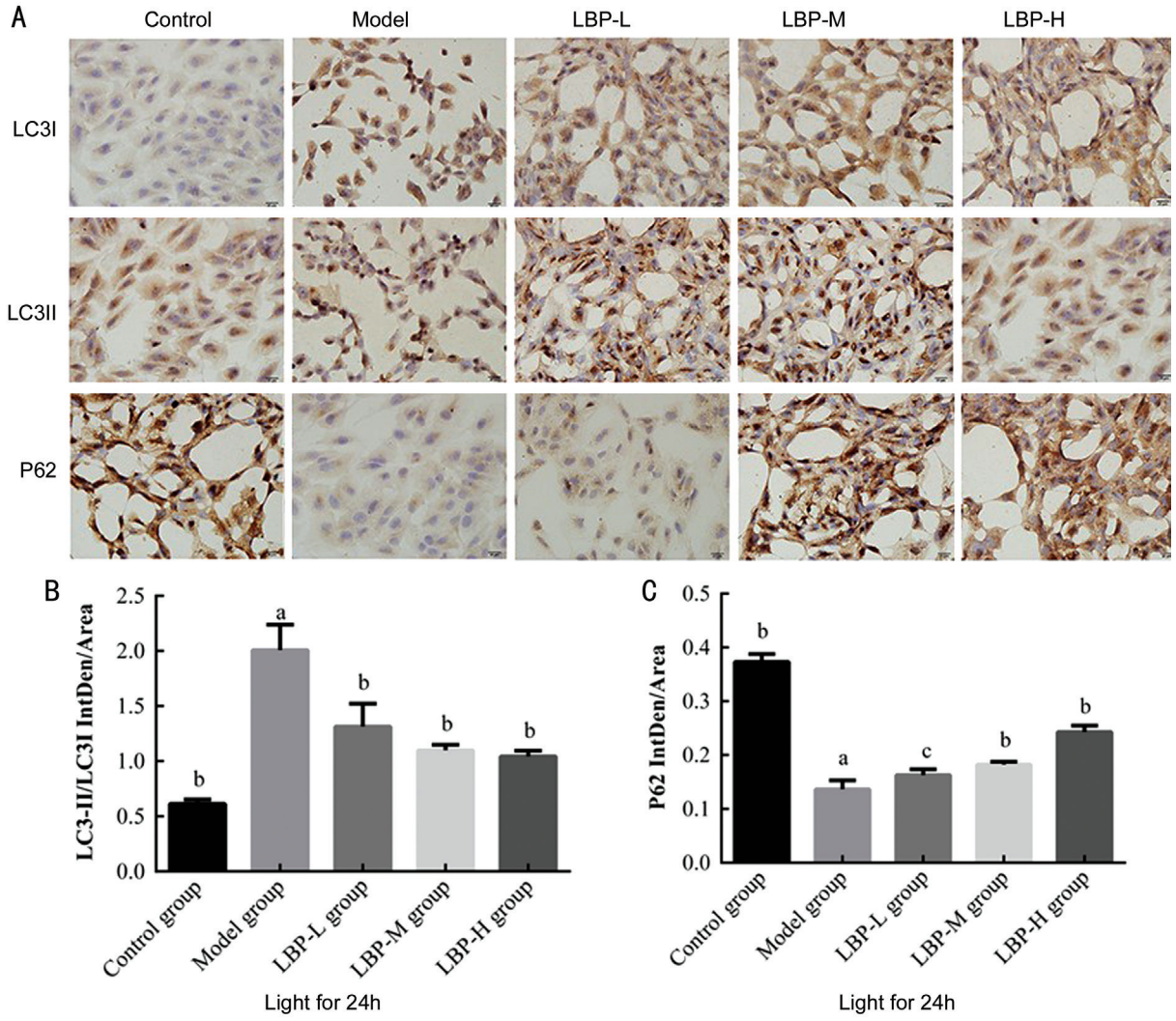

Figure 4 LBP inhibition of photoinduced autophagy in RPE cells was determined by immunofluorescence assay Compared with the control group, [a]$P<0.01$; compared with model group, [b]$P<0.01$, [c]$P<0.05$; $n=3$; results were expressed in mean±standard deviation.

as AMD. Degenerative changes in RPE cells are the major characteristics of AMD[21], and excessive illumination can accelerate the death of RPE cells and intensify the development of AMD. Furthermore, autophagy can damage RPE cells under

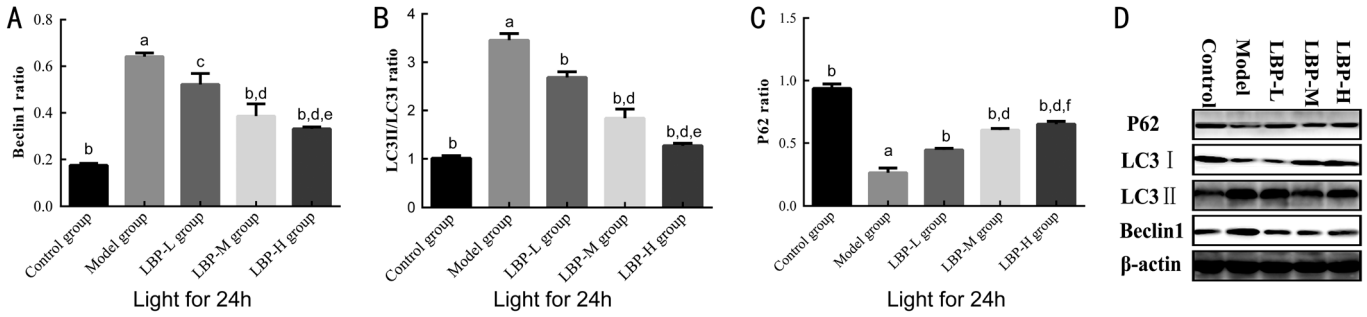

Figure 5 LBP inhibits photoinduced autophagy in ARPE-19 cells Compared with the control group, [a]P<0.01; compared with model group, [b]P<0.01, [c]P<0.05; compared with the LBP-L group, [d]P<0.01; compared with the LBP-M group, [e]P<0.01, [f]P<0.05; n=3, results are expressed as mean±standard deviation.

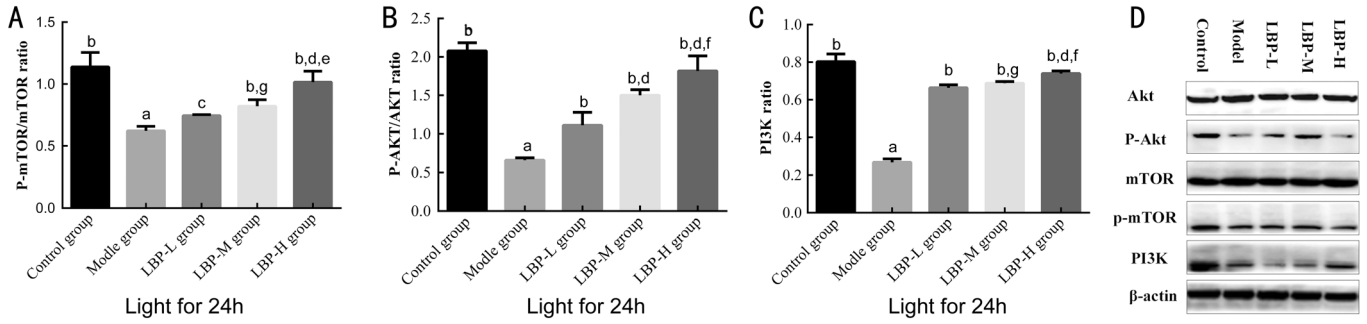

Figure 6 LBP activates the PI3K/AKt/mTOR signal pathway Compared with the control group, [a]P<0.01; compared with model group, [b]P<0.01, [c]P<0.05; compared with the LBP-L group, [d]P<0.01, [g]P>0.05; compared with the LBP-M group, [e]P<0.01, [f]P<0.05; n=3; results were expressed as mean±standard deviation.

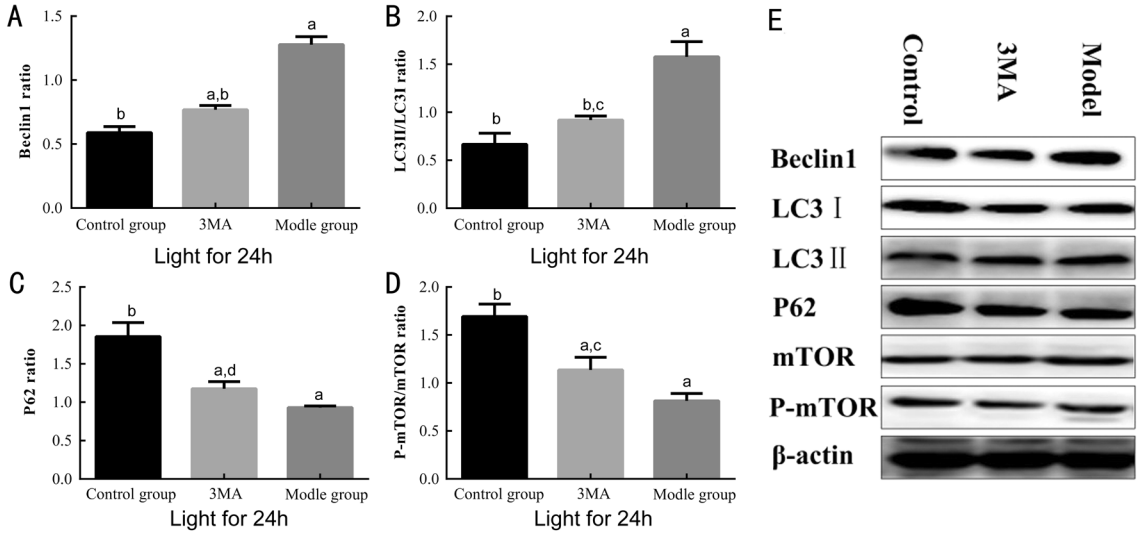

Figure 7 3MA inhibits the autophagy of ARPE-19 cells Compared with the control group , [a]P<0.01, [c]P<0.05; compared with model group, [b]P<0.01, [d]P<0.05; n=3, results are expressed as mean±standard deviation.

photoinduction, and inhibiting autophagy has a protective effect on RPE cells damaged by photodamage-induced. This result conforms to the research conclusions of Song *et al*[22], that might be a potential therapeutic strategy for early AMD.

Beclin 1 is an important factor in the formation of autophagosomes and is formed for positively regulated autophagy[23]. LC3 is the most classical autophagic molecular marker[24] and can realize target location in autophagosomes. When autophagy is activated, LC3-I in the cytoplasm is transformed into LC3-II in membrane bonding form. In general, increasing LC3-II or LC3II/I level indicates the formation of autophagy[25] and reflects strengthened autophagy in cells. P62 is an ubiquitination substrate associated with LC3 and integrated into autophagosomes. P62 binds with lysosomes to form autolysosomes. When autophagy is activated, organelles, such as P62, in autophagy vesicles are degraded, and the expression level of P62 decreases[26]; otherwise, the expression level of P62 increases when autophagy is inhibited.

In this experiment, ARPE-19 cells were exposed to 16500±500 lx of illumination. According to TEM observation, classical dual-membrane autophagosome was present in the ARPE-19 cells of the model group, indicating that illumination at this intensity can induce autophagy in ARPE-19 cells. The expression level of beclin1, which was an autophagy marker, in the model group increases significantly (P<0.01), and LC3II/I level is increased (P<0.01), whereas the expression level of P62 was low (P<0.01). After 24h of intervention was performed on photoinduced RPE cells with different concentrations of LBP, the survival rate was higher than that of the model group (P<0.01). According to flow cytometry, the LBP-L, LBP-M, and LBP-H groups showed lower levels of apoptosis than the model group (P<0.01). Moreover, compared with the model group, the dependence of LC3II/I and expression level of beclin1 on LBP dosage in the LBP-L, LBP-M, and LBP-H group decrease (P<0.05), and the expression level of P62 increased (P<0.05). These results showed that LBP can inhibit the apoptosis of the ARPE-19 in the model group and dosage dependence decreased the autophagy levels of ARPE-19 cells. The detection of LC3II/I and expression level of P62 with the cell immunofluorescence method further proved that LBP can inhibit autophagy in ARPE-19 cells and protect ARPE-19 cells from photodamage.

The PI3K/Akt/mTOR signal pathway plays an important role in the survival, proliferation, apoptosis, and autophagy of cells. The PI3K/Akt/mTOR signal pathway can weaken autophagy[27-29], and inhibit cell apoptosis[29]. Thus, the effects of LBP on autophagy and apoptosis in ARPE-19 cells were discussed preliminarily. Moreover, how LBP protects ARPE-19 cells through the PI3K/Akt/mTOR signaling pathway in the photoinduced *in vitro* ARPE-19 cell model was explored. The expression level of PI3K in the model group decreased compared with that of the control group (P<0.01), and P-mTOR/mTOR and P-Akt/Akt levels were low (P<0.01). Moreover, PI3K, P-mTOR/mTOR, and P-Akt/Akt levels in the LBP-L, LBP-M, and LBP-H groups increased relative to those in the model group (P<0.01). These data showed that LBP can protect RPE cells from photodamage, and such protective effect was related to the activation of the PI3K/Akt/mTOR signaling pathway.

As a PI3K inhibitor, 3MA is extensively used in studies on autophagy. In the present study, 3MA was used in processing cells. The expression levels of LC3II/I and beclin1 in the 3MA group increased slightly, whereas the expression level of P62 decreased relative to those in the control group. Moreover, the expression levels of LC3II/I and beclin1 in the 3MA group are decreased, but the expression level of P62 is increased compared with those of the model group. These results further demonstrated that 3MA inhibits photoinduced excessive autophagy in ARPE-19 cells.

According to our previous studies, LBP is involved in the PI3K/Akt/mTOR signaling pathway and can inhibit the formation of reactive oxygen species and malonaldehyde (MDA) and oxidative stress to protect cells from photodamage. Oxidative stress can activate the autophagy of nerve cells and is thus conducive to the decomposition of macromolecules and collection of their components. This feature retains cell energy and eliminates damaged proteins and mitochondria[30]. However, long-term autophagy can cause cell apoptosis[31]. This study further discussed. LBP could protect cells by inhibiting excessive autophagy. LBP might protect ARPE-19 from photodamage by inhibiting cell apoptosis and autophagy. To protect RPE cells from photodamage, LBP promotes the phosphorylation of mTOR and Akt, thus activating the PI3K/AKt/mTOR signaling pathway and inhibiting autophagy. However, LBP may also protect RPE cells from photodamage through other pathways, and this possibility deserves further study.

ACKNOWLEDGEMENTS

Authors' contributions: Gao YY performed the review, analyzed the data, and wrote and edited the manuscript. Yu Y, Li J, Huang J, and Li WJ each contributed to writing and editing of the manuscript.

Foundations: Supported by National Natural Science Foundation of China (No.82060885); Ningxia Scientific Research Program for Institution of Higher Education (No.NGY2018-99); Ningxia Natural Science Foundation (No.2020AAC03172).

Conflicts of Interest: Gao YY, None; **Li J,** None; **Huang J,** None; **Li WJ,** None; **Yu Y,** None.

REFERENCES

1 Hammoutene A, Biquard L, Lasselin J, Kheloufi M, Tanguy M, Vion AC, Mérian J, Colnot N, Loyer X, Tedgui A, Codogno P, Lotersztajn S, Paradis V, Boulanger CM, Rautou PE. A defect in endothelial autophagy occurs in patients with non-alcoholic steatohepatitis and promotes inflammation and fibrosis. *J Hepatol* 2020;72(3):528-538.

2 Devis-Jauregui L, Eritja N, Davis ML, Matias-Guiu X, Llobet-Navàs D. Autophagy in the physiological endometrium and cancer. *Autophagy* 2021;17(5):1077-1095.

3 Karim MR, Fisher CR, Kapphahn RJ, Polanco JR, Ferrington DA. Investigating AKT activation and autophagy in immunoproteasome-deficient retinal cells. *PLoS One* 2020;15(4):e0231212.

4 Zhang TZ, Fan B, Chen X, Wang WJ, Jiao YY, Su GF, Li GY. Suppressing autophagy protects photoreceptor cells from light-induced injury. *Biochem Biophys Res Commun* 2014;450(2):966-972.

5 Xie XM, Z XL, W J. The composition and analysis of Lycium barbarum polysaccharide. *Chinese Herbal Medicines* 2020(07):1649-1652.

6 Zhang G, Chen SS, Zhou W, *et al*. The function research and research progress of Lycium ruthenicum. *West China Journal of Pharmaceutical Sciences* 2019;34(06):638-642.

7 He MH, Pan H, Chang RC, So KF, Brecha NC, Pu ML. Activation of the Nrf2/HO-1 antioxidant pathway contributes to the protective effects of Lycium barbarum polysaccharides in the rodent retina after ischemia-reperfusion-induced damage. *PLoS One* 2014;9(1):e84800.

8 Lakshmanan Y, Wong FSY, Zuo B, So KF, Bui BV, Chan HH. Posttreatment intervention with lycium barbarum polysaccharides is neuroprotective in a rat model of chronic ocular hypertension. *Invest Ophthalmol Vis Sci* 2019;60(14):4606-4618.

9 Pop C, Berce C, Ghibu S, Scurtu I, Soriţău O, Login C, Kiss B, Ştefan MG, Fizeşan I, Silaghi H, Mocan A, Crişan G, Loghin F, Mogoşan C. Effects of *Lycium barbarum* L. polysaccharides on inflammation and oxidative stress markers in a pressure overload-induced heart failure rat model. *Molecules* 2020;25(3):E466.

10 Wu W, Xue SJ, Zhu LQ, *et al*. Study on the protective effect of Lycium barbarum polysaccharides on hydrogen peroxide-induced vascular endothelial cell injury through antioxidant and anti-apoptotic effects. *Lishizhen Medicine and Materia Medica Research* 2019;30(05): 1047-1049.

11 Huang J. Effects of Lycium barbarum polysaccharides on light-induced oxidative stress damage of human retinal pigment epithelial cells and PI3K/Akt/mTOR signaling pathway. *Ningxia Medical University* 2020.

12 Huang J, Gao YY, Zhao FF, *et al*. Effects of Lycium barbarum polysaccharides on light-induced oxidative stress in human RPE cells. *Hubei Journal of Traditional Chinese Medicine* 2019;41(08):7-11.

13 Zhao FF, Yang DP, Yu Y. Effects of Lycium barbarum polysaccharides on the signal transduction pathway of apoptotic mitochondria in rabbit retinal pigment epithelial cells with light damage. *Hubei Journal of Traditional Chinese Medicine* 2018,40(10):3-8.

14 Song C, Yu Y. Effect of Lycium barbarum-containing serum on the signal transduction pathway of apoptotic mitochondria in rabbit retinal pigment epithelial cells after light damage. *Liaoning Journal of Traditional Chinese Medicine* 2016,43(11):2410-2414.

15 Song C, Yu Y. Effects of different light duration on photo-damaged apoptosis of human retinal pigment epithelial cells *in vitro*. *Journal of Ningxia Medical University* 2014;36(06):592, 625-627, 637.

16 Yu Y, Feng ZE, Li N, Jiang H. Experimental study on protective effect of wolfberry fruit serum on light damage of rabbit retinal pigment epithelial cells. *Chinese Journal of Traditional Chinese Medicine* 2012,27(11):2950-2952.

17 Huang J, Gao YY, Zhao FF, *et al*. Protective effect and mechanism of Lycium barbarum polysaccharides on light-induced damage of human retinal pigment epithelial cells. *Lishizhen Medicine and Materia Medica Research* 2019;30(12):2870-2872.

18 Zhang LM, Zhou YY, Xia QQ, Chen Y, Li J. All-trans-retinal induces autophagic cell death *via* oxidative stress and the endoplasmic reticulum stress pathway in human retinal pigment epithelial cells. *Toxicol Lett* 2020;322:77-86.

19 Feng H. Autophagy resistant cell epithelial-mesenchymal phenotypic transformation process maintains retinal pigment epithelium homeostasis. *China Medical University* 2019.

20 Lakkaraju A, Umapathy A, Tan LX, Daniele L, Philp NJ, Boesze-Battaglia K, Williams DS. The cell biology of the retinal pigment epithelium. *Prog Retin Eye Res* 2020:100846.

21 Wang SB, Wang XR, Cheng YQ, Ouyang WJ, Sang X, Liu JH, Su YR, Liu Y, Li CY, Yang L, Jin L, Wang ZC. Autophagy dysfunction, cellular senescence, and abnormal immune-inflammatory responses in AMD: from mechanisms to therapeutic potential. *Oxid Med Cell Longev* 2019;2019:3632169.

22 Song JY, Fan B, Che L, Pan YR, Zhang SM, Wang Y, Bunik V, Li GY. Suppressing endoplasmic reticulum stress-related autophagy attenuates retinal light injury. *Aging* (*Albany NY*) 2020;12(16):16579-16596.

23 Zhang LM, Xia QQ, Zhou YY, Li J. Endoplasmic reticulum stress and autophagy contribute to cadmium-induced cytotoxicity in retinal pigment epithelial cells. *Toxicol Lett* 2019;311:105-113.

24 Schaaf MB, Keulers TG, Vooijs MA, Rouschop KM. LC3/GABARAP family proteins: autophagy-(un)related functions. *FASEB J* 2016;30(12):3961-3978.

25 Kaarniranta K, Uusitalo H, Blasiak J, Felszeghy S, Kannan R, Kauppinen A, Salminen A, Sinha D, Ferrington D. Mechanisms of mitochondrial dysfunction and their impact on age-related macular degeneration. *Prog Retin Eye Res* 2020;79:100858.

26 Zhong Y, Morris DH, Jin L, Patel MS, Karunakaran SK, Fu YJ, Matuszak EA, Weiss HL, Chait BT, Wang QJ. Nrbf2 protein suppresses autophagy by modulating Atg14L protein-containing Beclin 1-Vps34 complex architecture and reducing intracellular phosphatidylinositol-3 phosphate levels. *J Biol Chem* 2014;289(38): 26021-26037.

27 Yu Y, Wu XQ, Pu JN, Luo P, Ma WK, Wang J, Wei JL, Wang YX, Fei Z. Lycium barbarum polysaccharide protects against oxygen glucose deprivation/reoxygenation-induced apoptosis and autophagic cell death *via* the PI3K/Akt/mTOR signaling pathway in primary cultured hippocampal neurons. *Biochem Biophys Res Commun* 2018;495(1):1187-1194.

28 Shi GJ, Zheng J, Han XX, Jiang YP, Li ZM, Wu J, Chang Q, Niu Y, Sun T, Li YX, Chen Z, Yu JQ. Lycium barbarum polysaccharide attenuates diabetic testicular dysfunction *via* inhibition of the PI3K/Akt pathway-mediated abnormal autophagy in male mice. *Cell Tissue Res* 2018;374(3):653-666.

29 Song SQ, Lin FL, Zhu PY, Wu CY, Zhao SL, Han Q, Li XM. *Lycium barbarum* polysaccharide alleviates oxygen glucose deprivation-induced PC-12 cells damage by up-regulating miR-24. *Artif Cells Nanomed Biotechnol* 2019;47(1):3994-4000.

30 Zhu YC, Tang QQ, Wang GP, Han RD. Tanshinone IIA protects hippocampal neuronal cells from reactive oxygen species through changes in autophagy and activation of phosphatidylinositol 3-kinase, protein kinas B, and mechanistic target of rapamycin pathways. *Curr Neurovasc Res* 2017;14(2):132-140.

31 Laha D, Deb M, Das H. KLF2 (kruppel-like factor 2 [lung]) regulates osteoclastogenesis by modulating autophagy. *Autophagy* 2019;15(12): 2063-2075.